Preparation, Molecular and Electronic Structures, and Magnetic Properties of Face-Sharing Bioctahedral Titanium(III) Compounds: $[PPh_4][Ti_2(\mu\text{-}Cl)_3Cl_4(PR_3)_2]$

Linfeng Chen,[†] F. Albert Cotton,*[,†] Kim R. Dunbar,[‡] Xuejun Feng,[†] Robert A. Heintz,[‡] and Calvin Uzelmeir[‡]

Department of Chemistry and Laboratory for Molecular Structure and Bonding, Texas A&M University, College Station, Texas 77843, and Department of Chemistry, Michigan State University, East Lansing, Michigan 48824

Received May 30, 1996[⊗]

Reduction of $TiCl_4$ with 1 equiv of $HSnBu_3$ followed by addition of $[PPh_4]Cl$ and then PR_3 leads to two new dinuclear titanium(III) compounds, $[PPh_4][Ti_2(\mu\text{-}Cl)_3Cl_4(PR_3)_2]$ (R = Et and $R_3 = Me_2Ph$), both of which contain an anion with the face-sharing bioctahedral type structure. Their crystal structures are reported. $[PPh_4][Ti_2(\mu\text{-}Cl)_3Cl_4(PEt_3)_2]\cdot 2CH_2Cl_2$ crystallized in the triclinic space group $P\bar{1}$. Cell dimensions: $a = 12.461(1)$ Å, $b = 20.301(8)$ Å, $c = 11.507(5)$ Å, $\alpha = 91.44°$, $\beta = 113.27(1)°$, $\gamma = 104.27(2)°$, and $Z = 2$. The distance between titanium atoms is 3.031(2) Å. $[PPh_4][Ti_2(\mu\text{-}Cl)_3Cl_4(PMe_2Ph)_2]\cdot CH_2Cl_2$ also crystallized in the triclinic space group $P\bar{1}$ with cell dimensions $a = 11.635(4)$ Å, $b = 19.544(3)$ Å, $c = 11.480(3)$ Å, $\alpha = 100.69(2)°$, $\beta = 109.70(1)°$, $\gamma = 95.08(2)°$, and $Z = 2$. The distance between titanium atoms in this compound is 2.942(1) Å. Variable temperature magnetic susceptibilities were measured for $[PPh_4][Ti_2(\mu\text{-}Cl)_3Cl_4(PEt_3)_2]$. Electronic structure calculations were carried out for a model ion, $[Ti_2(\mu\text{-}Cl)_3Cl_4(PH_3)_2]^-$, and another well-known anion, $[Ti_2(\mu\text{-}Cl)_3Cl_6]^{3-}$, by employing an *ab initio* configuration interaction method. The results of the calculations reveal that the metal−metal interaction in these Ti(III) face-sharing compounds can be best described by strong antiferromagnetic coulping that leads to a singlet ground state and a thermally accessible triplet first excited state. Accordingly the measured magnetic data were satisfactorily fitted to a spin-only formula.

Introduction

Titanium has a marked tendency to form cluster species that possess bridging halogen atoms.[1] One important class of dinuclear titanium(III) complex are those with a structure of two fused octahedra that share a common edge. Many such edge-sharing bioctahedral compounds have been synthesized and crystallographically characterized.[2] Another important class comprises those in which two titanium atoms are bridged by three halogen atoms as to form a face-sharing bioctahedron, exemplified by the two dinuclear Ti(IV) compounds $[(C_6Me_6)TiCl_3][Ti_2(\mu\text{-}Cl)_3Cl_6]$[3] and $[PCl_4][Ti_2(\mu\text{-}Cl)_3Cl_6]$,[4] both of which contain a crystallographically characterized bioctahedral $[Ti_2(\mu\text{-}Cl)_3Cl_6]^-$ ion. Dinuclear Ti(III) compounds that exhibit the face-sharing bioctahedral structure are unknown, except for the solid state salts, $A_3Ti_2X_9$ (A = Cs, Rb, Et_2NH_2; X = Cl, Br),[5−8] which contain a $[Ti_2(\mu\text{-}X)_3X_6]^{3-}$ anion. It has long been known that the crystal structures of these salts are isomorphous with that of $Cs_3Cr_2Cl_9$,[5] but full structural characterization has never been formally reported.[7] The $[Ti_2Cl_9]^{3-}$ ion has been extensively studied for its spectroscopic and, in particular, magnetic properties.[6−10] Interest in the latter stems from the high symmetry (D_{3h}) of the anion and its simple d^1-d^1 electronic configuration, which renders it an ideal candidate for studying magnetic exchange interaction between two metal centers with orbitally degenerate local ground states where unquenched orbital angular momenta are involved.[7−10]

Recent studies in this laboratory involving titanium chemistry have led to a number of new types of titanium compounds. Herein we report the synthesis and characterization of two new dinuclear Ti(III) compounds, namely, $[PPh_4][Ti_2(\mu\text{-}Cl)_3Cl_4(PEt_3)_2]$ and $[PPh_4][Ti_2(\mu\text{-}Cl)_3Cl_4(PMe_2Ph)_2]$. These compounds, which both contain a $[Ti_2Cl_7(PR_3)_2]^-$ anion with the face-sharing bioctahedral structure, constitute the first Ti(III) compounds of this type to have been fully characterized by X-ray crystallography. In addition to the synthetic and structural significance, magnetic properties of these new compounds will also be of great interest since they provide an instructive comparison to those of $[Ti_2Cl_9]^{3-}$. The variable temperature magnetic susceptibilities have therefore been measured for one of the compounds, namely, $[PPh_4][Ti_2Cl_7(PEt_3)_2]$. In conjunction with

[†] Texas A&M University.
[‡] Michigan State University.
[⊗] Abstract published in *Advance ACS Abstracts,* November 1, 1996.

(1) (a) Bottrill, M.; Gavens, P. D.; McMeeking, J. Low Valent Complexes of Titanium. In *Comprehensive Organometallic Chemistry*; Wilkinson, G., Stone, F. G. A., Abel, E. W., Eds.; Pergamon Press: Oxford, England, 1982; Vol. 3, Chapter 22.2. (b) McAuliffe, C. A.; Barratt, D. S. Titanium. In *Comprehensive Coordination Chemistry*; Wilkinson, G., Gillard, R. D., McCleverty, J. A., Eds.; Pergamon Press: Oxford, England, 1987; Vol. 3, Chapter 31.
(2) (a) Cotton, F. A.; Wojtczak, W. A. *Gazz. Chim. Ital*. **1993**, *123,* 499. (b) Solari, E.; Floriani, C.; Schenk, K. *J. Chem. Soc., Chem. Commun*. **1990**, 963. (c) Sobota, P.; Ejfler, J.; Utko, J.; Lis, T. *J. Organomet. Chem*. **1991**, *410*, 149. (d) Quinkert, G.; del Grosso, M.; Bucher, A.; Bauch, M.; Doring, W.; Bats, J. W.; Durner, G. *Tetrahedron Lett*. **1992**, *33*, 3617. (e) Hill, J. E.; Nash, J. M.; Fanwick, P. E.; Rothwell, I. P. *Polyhedron*, **1990**, *9*, 1617. (f) Dieck, H. T.; Rieger, H. J.; Fendesak, G. *Inorg. Chim. Acta* **1990,** *177,* 191. (g) Sobota, P.; Ejfler, J.; Szafert, S.; Szczegot, K.; Sawaka-Dobrowlska, W. *J. Chem. Soc., Dalton Trans.* **1993**, 2535.
(3) Solari, E.; Floriani, C.; Chiesi-Villa, A.; Guastini, C. *J. Chem. Soc., Chem. Commun*. **1989,** 1747.
(4) Kistenmacher, T. J.; Stucky, G. D. *Inorg. Chem*. **1971**, *10,* 122.
(5) (a) Wessel, G. J.; Ijdo, D. J. W. *Acta Crystallogr*., **1957**, *10*, 446. (b) Kozhina, I. I.; Korol'kov, D. V. *Zh. Strukt. Khim*. **1965**, *6*, 97.
(6) Crouch, P. C.; Fowles, G. W. A.; Walton, R. A. *J. Chem. Soc. A* **1969**, 972.
(7) Briat, B.; Kahn, O.; Morgenstern-Badarau, I.; Rivoal, J. C. *Inorg. Chem*. **1981**, *20*, 4193.
(8) Leuenberger, B.; Gudel H. U.; Furrer, A. *Chem. Phys. Lett*. **1986**, *126*, 255.
(9) Drillon, M.; Georges R. *Phys. Rev. B* **1982**, *26*, 3882.
(10) Kahn, O. *Molecular Magnetism*; VCH: New York, 1993, and references therein.

S0020-1669(96)00636-2 CCC: $12.00

the magnetic property investigation, electronic structure calculations were carried out by an *ab initio* method that includes configuration interaction (CI). Parallel calculations were also performed for the well-known $[Ti_2Cl_9]^{3-}$ ion, which has not been subjected to any previous *ab initio* computational studies. In this paper, these magnetic and theoretical results are reported and discussed for both the $[Ti_2Cl_9]^{3-}$ and $[Ti_2Cl_7(PR_3)_2]^-$ complexes.

Experimental Section

All manipulations were conducted under an argon atmosphere. Glassware was oven dried at 150 °C for 24 h prior to use. Solvents were predried over molecular sieves and freshly distilled under nitrogen from appropriate drying reagents. $TiCl_4$, $HSnBu_3$, $[PPh_4]Cl$, PEt_3, and PMe_2Ph were purchased from Aldrich and used as received except for $[PPh_4]Cl$, which was dried at 150 °C under vacuum for 24 h.

Preparation of $[PPh_4][Ti_2Cl_7(PEt_3)_2]$ (1). To a solution of 0.22 mL (2.0 mmol) of $TiCl_4$ in 20 mL of toluene was added dropwise 0.54 mL (2.0 mmol) of $HSnBu_3$. A gray-green precipitate was observed to form instantaneously. After the reaction mixture had been stirred at room temperature for 2 h, the solution was decanted and the precipitate was washed with two 10 mL portions of toluene. Residual solvent was removed from the precipitate by evaporation under a dynamic vacuum. Then 375 mg (1.0 mmol) of $[PPh_4]Cl$ in 15 mL of CH_2Cl_2 was slowly added to the precipitate via a cannula with stirring. A dark green solid was observed to form on the wall of the flask. After 30 min, the solution was decanted and the solid was washed with 2×10 mL of CH_2Cl_2. Then 10 mL of CH_2Cl_2 and 0.30 mL (2.0 mmol) of PEt_3 were added dropwise through a syringe to give a green solution. The solution was filtered and layered with 30 mL of hexane which led to the production of large, plate-shaped, dark green crystals of **1**·$2CH_2Cl_2$ (76% yield) over a period of 2 weeks.

Preparation of $[PPh_4][Ti_2Cl_7(PMe_2Ph)_2]$ (2). This compound was synthesized in a similar way to that described for compound **1**. The yield for **2**·CH_2Cl_2 was 80%.

X-ray Crystallography. Crystals that were used in diffraction intensity measurements were mounted on the tip of a quartz fiber and placed in a cold stream of nitrogen. Diffraction measurements were made on an Enraf-Nonius FAST area-detector diffractometer with graphite-monochromated Mo Kα radiation. For each crystal, preliminary data collection was carried out first to produce all parameters and an orientation matrix. Fifty reflections were used in indexing and 250 reflections in cell refinement. Axial images were obtained to determined the Laue groups and cell dimensions. No decay corrections or absorption corrections were applied.[11]

Each structure was solved by a combination of direct methods using SHELXS-86 program[12a] and difference Fourier analyses using SHELXL-93.[12b] Crystallographic data and results are listed in Table 1.

$[PPh_4][Ti_2Cl_7(PEt_3)_2]$·$2CH_2Cl_2$ crystallizes in the triclinic crystal system. The space group $P\bar{1}$ (No. 2) was assumed and confirmed by successful solution and refinement of the structure. Two ethyl groups in each PEt_3 ligand were found to be disordered between two positions. Their occupancies were refined as 42% and 58%, 44% and 56%, 44% and 56%, and 36% and 64%. Except for the disordered carbon atoms, all non-hydrogen atoms were refined with anisotropic thermal parameters. The disordered atoms were refined isotropically with constraints of distances of P−C = 1.83(2) Å and C−C = 1.519(2) Å. The positions of hydrogen atoms were calculated by assuming idealized geometries, C−H = 0.98 Å in methyl groups, C−H = 0.97 Å in methylene groups, and C−H = 0.94 Å in phenyl groups. They were refined with thermal parameters of $1.5B_{eq}$ of the corresponding carbon atoms for the methyl groups and $1.2B_{eq}$ for the other groups.

$[PPh_4][Ti_2Cl_7(PMe_2Ph)_2]$·$CH_2Cl_2$ also crystallizes in the triclinic crystal system. The space group $P\bar{1}$ (No. 2) was assumed and confirmed by successful solution and refinement of the structure. All non-hydrogen atoms were refined anisotropically. The hydrogen atoms were treated as described in the previous section for $[PPh_4][Ti_2Cl_7(PEt_3)_2]$·$2CH_2Cl_2$.

Table 1. Crystal Data for Compounds **1**·$2CH_2Cl_2$ and **2**·CH_2Cl_2

	1·$2CH_2Cl_2$	**2**·CH_2Cl_2
formula	$C_{38}H_{54}Cl_{11}P_3Ti_2$	$C_{41}H_{44}Cl_{19}P_3Ti_2$
fw	1089.47	1044.52
cryst syst	triclinic	triclinic
space group	$P\bar{1}$	$P\bar{1}$
a, Å	12.461(1)	11.635(4)
b, Å	20.301(8)	19.544(3)
c, Å	11.507(5)	11.480(3)
α, deg	91.44(1)	100.69(2)
β, deg	113.27(1)	109.70(1)
γ, deg	104.27(2)	95.08(2)
V, Å^3	2567(2)	2383(1)
Z	2	2
d_{calc}, g/cm^3	1.410	1.456
μ, cm^{-1}	10.03	9.70
temp, °C	−60	−100
$2\theta_{max}$, deg	50	50
no. of observns ($I > 2\sigma(I)$)	5654	7853
no. of variables	493	672
residuals: R1,[a] wR2[b]	0.061, 0.144	0.050, 0.120
quality-of-fit indicator[c]	1.064	1.095

[a] $R1 = \sum||F_o| - |F_c||/\sum|F_o|$ (based on reflections with $F_o^2 > 2\sigma F_o^2$). [b] $wR2 = [\sum[w(F_o^2 - F_c^2)^2]/\sum[w(F_o^2)^2]]^{1/2}$; $w = 1/[\sigma^2(F_o^2) + (0.095P)^2]$; $P = [\text{Max}(F_o^2, 0) + 2F_c^2]/3$ (also with $F_o^2 > 2\sigma F_o^2$). [c] Quality-of-fit (on F^2) $= [\sum[w(F_o^2 - F_c^2)^2]/(N_{observns} - N_{params})]^{1/2}$.

Magnetic Measurements. The magnetic susceptibility data were collected on a Quantum Design, Model MPMS, SQUID (superconducting quantum interference device) for $[PPh_4][Ti_2Cl_7(PEt_3)_2]$·$2CH_2Cl_2$. The microcrystalline sample (several large crystals carefully broken up with a spatula (not ground with a mortar and pestle)) was loaded into a sample holder inside a nitrogen glovebag. The sample was protected from air exposure and transferred quickly into the SQUID. Data were collected from 5 to 320 K at a field of 1000 G. The molar susceptibilities were corrected for diamagnetism of the complex by using a sum of Pascal's constants.

Computational Procedures. Electronic structure calculations were performed for two ionic compounds, namely, $[Ti_2Cl_7(PH_3)_2]^-$ and $[Ti_2Cl_9]^{3-}$, both of which have a face-sharing bioctahedral structure. The structural parameters used in the calculations for $[Ti_2Cl_7(PH_3)_2]^-$ were obtained from the crystal structure data for $[PPh_4][Ti_2Cl_7(PEt_3)_2]$ and were idealized to conform to C_{2v} symmetry. Distances and angles for $[Ti_2Cl_9]^{3-}$ of D_{3h} molecular symmetry were taken from a footnote in reference 7, namely, Ti−Ti = 3.19 Å, Ti−Cl(bridging) = 2.50 Å, Ti−Cl(terminal) = 2.33 Å, and Cl(terminal)−Ti−Cl(terminal) = 95°.

The *ab initio* CI calculations utilized effective core potentials (ECP) so that only the outermost valence electrons of each atom were treated explicitly. For titanium, these are the electrons in 3d, 4s and 4p orbitals, and for chlorine and phosphorus these are the 3s and 3p electrons. We used the ECPs of Hay and Wadt and their valence Gaussian basis functions.[13] For Ti, the (3s2p6d) basis set was contracted to a (2s2p3d) set, and for Cl and P the (3s3p) basis to a double-ζ (2s2p) set. For hydrogen, a double-ζ basis set was used.

A three-step procedure was employed in the configuration interaction calculations in which the orbitals for the final CI expansions were optimized separately for the ground state and all triplet states through two steps of CI calculations. We started with the first step CI for all states being optimized over the same limited set of 34 valence molecular orbitals occupied by 26 electrons which includes the metal−ligand bonding and antibonding orbitals and metal-based orbitals. The MOs were obtained from an open-shell restricted Hartree−Fock (ORHF) calculation on the triplet state characterized by the $\sigma^1\sigma^{*1}$ configuration. Natural orbitals derived from this CI with occupation number less than 1.99 together with all remaining ORHF virtual orbitals were then used to form the active orbital space for the second stage CI optimization. The reference configurations for these CI optimizations involved occupations of both bonding and antibonding combinations of metal orbitals. For example, two references were used for the singlet ground

(11) Sheidt, W. R.; Turowska-Tyrk, I. *Inorg. Chem.* **1994**, *33*, 1314.
(12) (a) Sheldrick, G. M. SHELXS-86 Program for Crystal Structure Determination. University of Cambridge, England, 1986. (b) Sheldrick G. M. SHELXL-93 Program for Crystal Stucture Refinement. University of Göttingen, Germany, 1993.
(13) Hay, P. J.; Wadt, W. R. *J. Chem. Phys.* **1985**, *82*, 270, 284, and 299.

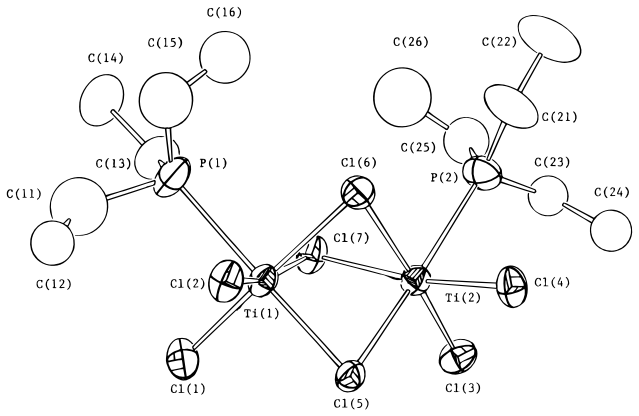

Figure 1. Molecular structure of $[Ti_2(\mu\text{-}Cl)_3Cl_4(PEt_3)_2]^-$ in $[PPh_4][Ti_2(\mu\text{-}Cl)_3Cl_4(PEt_3)_2]$ showing 50% probability thermal ellipsoids.

Scheme 1

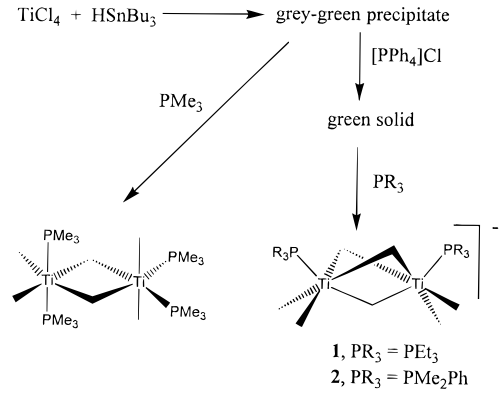

1, $PR_3 = PEt_3$
2, $PR_3 = PMe_2Ph$

state, namely, $\sigma^2\sigma^{*0}$ and $\sigma^0\sigma^{*2}$, two for an excited $^3B_1$ (in C_{2v} symmetry), namely, $\sigma^1\pi^1$ and $\sigma^{*1}\pi^{*1}$, but only one, $\sigma^1\sigma^{*1}$, for the triplet first excited state $^3A_2''$ (or $^3B_2$ in C_{2v}). The final CI calculations were carried out by using all natural orbitals obtained from the second step CI and the same reference configurations. The active space for the CI of the last two steps includes 10 electrons in 104 orbitals in the case of $[Ti_2Cl_7(PH_3)_2]^-$, and 10 electrons in 92 orbitals for $[Ti_2Cl_9]^{3-}$. In all CI calculations, all symmetry-allowed single and double excitations out of the reference configurations were included in the CI wave functions. CI calculations for all other singlet states used natural orbitals optimized for the their corresponding triplet states.

All calculations were performed by the GAMESS program package[14] on a SGI Power Challenge XL computer at the Texas A&M University Supercomputer Center.

Results and Discussion

Synthesis and Structures. The reduction of $TiCl_4$ with $HSnBu_3$ yields a gray-green precipitate,[2a] presumably a polymeric Ti(III) compound,[2a] which when treated with PR_3 or $[RNCHNR]^-$ ligands produces edge-sharing bioctahedral compounds of the type $Ti_2(\mu\text{-}Cl)_2Cl_4(PR_3)_4$ and $Ti_2(\mu\text{-}Cl)_2(RNCHNR)_4$. If the precipitate is first treated with $[PPh_4]Cl$, addition of PR_3 instead produces face-sharing compounds $[PPh_4][Ti_2Cl_7(PR_3)_2]$ (Scheme 1).

$[PPh_4][Ti_2Cl_7(PEt_3)_2]\cdot 2CH_2Cl_2$ was characterized by single-crystal X-ray diffraction. The structure of the $[Ti_2Cl_7(PEt_3)_2]^-$ anion is shown in Figure 1. There is an approximately octahedral ligand environment around each titanium atom. The dinuclear compound consists of two such octahedra sharing a common triangular face so that the metal atoms are bridged by three Cl atoms. It can be seen that two phosphine ligands occupy *cis* positions with respect to the Ti_2 unit. Selected bond distances and angles are listed in Table 2. The distance between the two Ti atoms is 3.031(2) Å. It is significantly shorter than the corresponding distance, 3.439(6) Å, in $[PCl_4][Ti_2Cl_9]$.[4] It is also shorter than that (3.191 Å) in $Cs_3Ti_2Cl_9$.[7] The average distance between a Ti atom and a Cl atom that is *trans* to a phosphine ligand is slightly less than that between a Ti atom and other bridging Cl atoms, namely, 2.451(1) vs 2.479(9) Å. Both of these are shorter than those in the $Cs_3Ti_2Cl_9$ and $[PCl_4][Ti_2Cl_9]$ compounds, 2.503 and 2.50(1) Å, respectively. The Ti−Cl(terminal) bond length (2.327(2) Å) in $[Ti_2Cl_7(PEt_3)_2]^-$ is essentially the same as that (2.328 Å) in $Cs_3Ti_2Cl_9$, but considerably longer than that (2.213(6) Å) in $[PCl_4][Ti_2Cl_9]$. The average Ti−P bond length is 2.63(1) Å.

Table 2. Selected Bond Lengths (Å) and Angles (deg) for $\mathbf{1}\cdot 2CH_2Cl_2$[a]

Ti(1)···Ti(2)	3.031(2)	Ti(2)−Cl(4)	2.347(2)
Ti(1)−Cl(1)	2.308(2)	Ti(2)−Cl(5)	2.452(2)
Ti(1)−Cl(2)	2.337(2)	Ti(2)−Cl(6)	2.472(2)
Ti(2)−Cl(3)	2.316(2)	Ti(2)−Cl(7)	2.465(2)
Ti(1)−Cl(5)	2.451(2)	Ti(1)−P(1)	2.622(2)
Ti(1)−Cl(6)	2.506(2)	Ti(2)−P(2)	2.643(2)
Ti(1)−Cl(7)	2.475(2)		
Ti(1)−Cl(5)−Ti(2)	76.35(5)	Cl(1)−Ti(1)−P(1)	88.01(8)
Ti(2)−Cl(6)−Ti(1)	74.99(6)	Cl(2)−Ti(1)−P(1)	86.27(6)
Ti(2)−Cl(7)−Ti(1)	75.69(5)	Cl(7)−Ti(1)−P(1)	88.98(6)
Cl(2)−Ti(1)−Cl(7)	167.93(8)	Cl(6)−Ti(1)−P(1)	92.02(8)
Cl(1)−Ti(1)−Cl(6)	171.22(7)	Cl(3)−Ti(2)−Cl(4)	97.80(7)
Cl(4)−Ti(2)−Cl(7)	170.73(7)	Cl(3)−Ti(2)−Cl(5)	93.73(7)
Cl(3)−Ti(2)−Cl(6)	171.86(7)	Cl(4)−Ti(2)−Cl(5)	93.51(6)
Cl(5)−Ti(2)−P(2)	177.17(7)	Cl(3)−Ti(2)−Cl(7)	90.57(7)
Cl(5)−Ti(1)−P(1)	178.57(7)	Cl(5)−Ti(2)−Cl(7)	89.88(6)
Cl(1)−Ti(1)−Ti(2)	121.78(6)	Cl(4)−Ti(2)−Cl(6)	90.03(7)
Cl(2)−Ti(1)−Ti(2)	123.81(6)	Cl(5)−Ti(2)−Cl(6)	87.99(6)
P(1)−Ti(1)−Ti(2)	126.80(6)	Cl(7)−Ti(2)−Cl(6)	81.47(6)
Cl(3)−Ti(2)−Ti(1)	122.72(7)	Cl(3)−Ti(2)−P(2)	89.07(7)
Cl(4)−Ti(2)−Ti(1)	124.46(6)	Cl(4)−Ti(2)−P(2)	86.52(7)
P(2)−Ti(2)−Ti(1)	126.06(6)	Cl(7)−Ti(2)−P(2)	89.67(7)
Cl(1)−Ti(1)−Cl(2)	100.29(8)	Cl(6)−Ti(2)−P(2)	89.18(7)
Cl(1)−Ti(1)−Cl(5)	92.51(7)	Cl(5)−Ti(1)−Ti(2)	51.84(4)
Cl(2)−Ti(1)−Cl(5)	94.94(6)	Cl(7)−Ti(1)−Ti(2)	52.00(4)
Cl(1)−Ti(1)−Cl(7)	90.62(7)	Cl(6)−Ti(1)−Ti(2)	52.00(5)
Cl(5)−Ti(1)−Cl(7)	89.68(6)	Cl(5)−Ti(2)−Ti(1)	51.80(4)
Cl(2)−Ti(1)−Cl(6)	88.47(7)	Cl(7)−Ti(2)−Ti(1)	52.31(5)
Cl(5)−Ti(1)−Cl(6)	87.26(7)	Cl(6)−Ti(2)−Ti(1)	53.01(5)
Cl(7)−Ti(1)−Cl(6)	80.60(6)		

[a] Numbers in parentheses are estimated standard deviations in the least significant digits.

$[PPh_4][Ti_2Cl_7(PMe_2Ph)_2]\cdot CH_2Cl_2$ was also characterized by X-ray crystallography. The structure of the $[Ti_2Cl_7(PMe_2Ph)_2]^-$ anion is shown in Figure 2. Selected bond distances and angles are given in Table 3. The structure of the $[Ti_2Cl_7(PMe_2Ph)_2]^-$ ion is very similar to that of $[Ti_2Cl_7(PEt_3)_2]^-$. The distance between the two Ti atoms in the former, 2.942(1) Å, is about 0.09 Å shorter than that in the latter. Also observed are a shorter distance (2.433(5) Å) between a Ti atom and a bridging Cl atom *trans* to the PMe_2Ph ligands and the average distance between the Ti atoms and other bridging Cl atoms (2.462(3) Å). Other bond lengths and angles are comparable to those found in $[Ti_2Cl_7(PEt_3)_2]^-$.

Electronic Structures. A qualitative picture of electronic structure of the face-sharing bioctahedral complexes may be given in a simple molecular orbital approach as in the case of our previous study of a related pair of niobium compounds, namely, $[Nb_2Cl_9]^{3-}$ and $[Nb_2Cl_7(PR_3)_2]^-$.[15] Consider an octahedral $TiCl_6$ fragment of the dinuclear unit slightly distorted

(14) Guest, M. F.; Kendrick, J.; van Lenthe, J. H.; Schoeffel, K.; Sherwood, P. *GAMESS-UK, User's Guide and Reference Manual*; Compuing for Science Ltd., Daresbury Laboratory: Daresbury, England, 1994.
(15) Cotton, F. A.; Feng, X.; Gutlich, P.; Kohlhaas, T.; Lu, J.; Shang, M. *Inorg. Chem.* **1994,** *33*, 3055.
(16) Van Vleck, J. H. *The Theory of Electric and Magnetic Susceptibilities*; Oxford University: London, 1932.

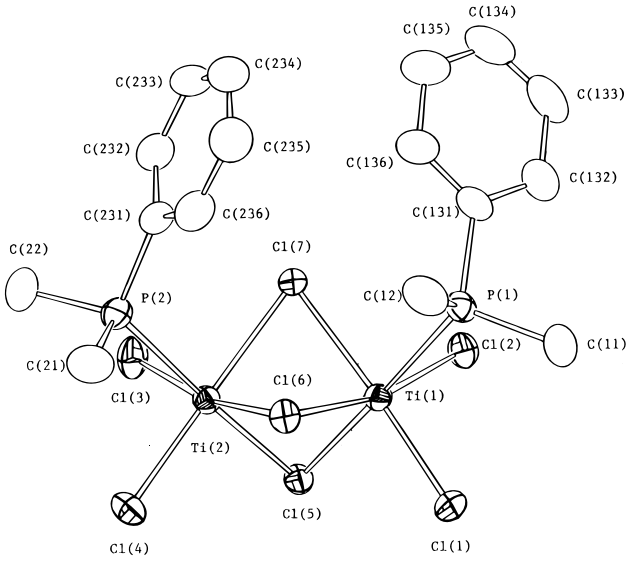

Figure 2. Molecular structure of $[Ti_2(\mu\text{-}Cl)_3Cl_4(PMe_2Ph)_2]^-$ in $[PPh_4][Ti_2(\mu\text{-}Cl)_3Cl_4(PMe_2Ph)_2]$ showing 50% probability thermal ellipsoids.

Table 3. Selected Bond Lengths (Å) and Angles (deg) for $\mathbf{2}\cdot CH_2Cl_2$[a]

Ti(1)···Ti(2)	2.942(1)	Ti(1)−Cl(7)	2.457(1)
Ti(1)−Cl(1)	2.313(1)	Ti(2)−Cl(5)	2.439(1)
Ti(1)−Cl(2)	2.347(1)	Ti(2)−Cl(6)	2.457(1)
Ti(2)−Cl(3)	2.345(1)	Ti(2)−Cl(7)	2.463(1)
Ti(2)−Cl(4)	2.336(1)	Ti(1)−P(1)	2.612(1)
Ti(1)−Cl(5)	2.428(1)	Ti(2)−P(2)	2.611(1)
Ti(1)−Cl(6)	2.471(1)		
Ti(1)−Cl(5)−Ti(2)	74.38(4)	Cl(1)−Ti(1)−P(1)	87.70(4)
Ti(2)−Cl(6)−Ti(1)	73.30(4)	Cl(2)−Ti(1)−P(1)	84.49(4)
Ti(1)−Cl(7)−Ti(2)	73.43(4)	Cl(7)−Ti(1)−P(1)	89.09(4)
Cl(1)−Ti(1)−Cl(7)	171.23(4)	Cl(6)−Ti(1)−P(1)	88.02(4)
Cl(2)−Ti(1)−Cl(6)	167.86(4)	Cl(4)−Ti(2)−Cl(3)	97.09(5)
Cl(5)−Ti(1)−P(1)	178.80(4)	Cl(4)−Ti(2)−Cl(5)	95.10(4)
Cl(3)−Ti(2)−Cl(6)	168.86(4)	Cl(3)−Ti(2)−Cl(5)	95.72(5)
Cl(4)−Ti(2)−Cl(7)	170.97(4)	Cl(4)−Ti(2)−Cl(6)	90.50(4)
Cl(5)−Ti(2)−P(2)	175.92(4)	Cl(5)−Ti(2)−Cl(6)	91.70(4)
Cl(1)−Ti(1)−Ti(2)	123.16(4)	Cl(3)−Ti(2)−Cl(7)	90.27(4)
Cl(2)−Ti(1)−Ti(2)	125.43(4)	Cl(5)−Ti(2)−Cl(7)	89.34(4)
P(1)−Ti(1)−Ti(2)	126.02(4)	Cl(6)−Ti(2)−Cl(7)	81.50(4)
Cl(4)−Ti(2)−Ti(1)	124.46(4)	Cl(4)−Ti(2)−P(2)	86.15(4)
Cl(3)−Ti(2)−Ti(1)	126.17(4)	Cl(3)−Ti(2)−P(2)	87.97(5)
P(2)−Ti(2)−Ti(1)	123.57(4)	Cl(6)−Ti(2)−P(2)	84.40(4)
Cl(1)−Ti(1)−Cl(2)	98.83(5)	Cl(7)−Ti(2)−P(2)	88.90(4)
Cl(1)−Ti(1)−Cl(5)	93.46(4)	Cl(5)−Ti(1)−Ti(2)	52.97(3)
Cl(2)−Ti(1)−Cl(5)	95.66(4)	Cl(7)−Ti(1)−Ti(2)	53.38(3)
Cl(2)−Ti(1)−Cl(7)	88.98(4)	Cl(6)−Ti(1)−Ti(2)	53.14(3)
Cl(5)−Ti(1)−Cl(7)	89.72(4)	Cl(5)−Ti(2)−Ti(1)	52.64(3)
Cl(1)−Ti(1)−Cl(6)	90.38(4)	Cl(6)−Ti(2)−Ti(1)	53.56(3)
Cl(5)−Ti(1)−Cl(6)	91.63(4)	Cl(7)−Ti(2)−Ti(1)	53.19(3)
Cl(7)−Ti(1)−Cl(6)	81.35(4)		

[a] Numbers in parentheses are estimated standard deviations in the least significant digits.

along one 3-fold axis of the octahedron. The octahedral t_{2g} nonbonding orbitals then split into a dσ orbital of lower energy and a doubly degenerate dπ orbital. When two such distorted octahedra fuse on a common triangular face to form a dinuclear molecule of D_{3h} symmetry, as in the case of $[Ti_2Cl_9]^{3-}$, the frontier molecular orbitals of the dinuclear species include bonding and antibonding linear combinations of the dσ orbitals, namely, σ and σ^* of a_1' and a_2'' symmetries, respectively, and of the dπ orbitals, namely, π and π^* of e′ and e″ symmetries, respectively. In the lower symmetry, C_{2v}, in the case of $[Ti_2Cl_7(PH_3)_2]^-$, the σ and σ^* orbitals would be labeled as a_1 and b_2, respectively, and the π (e′) and π^* (e″) orbitals split into a pair of a_1 and b_1 orbitals and a pair of b_2 and a_2 orbitals,

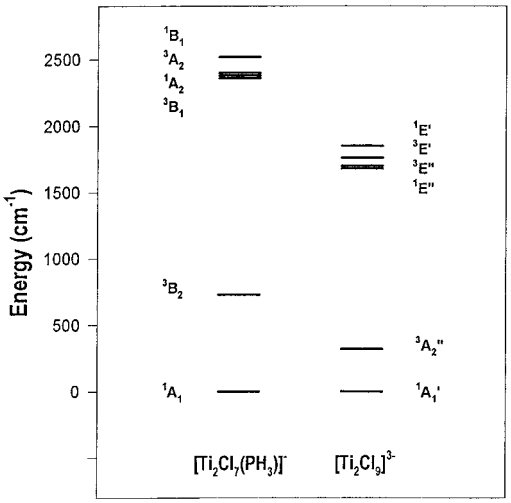

Figure 3. Total electronic energy diagrams for $[Ti_2Cl_7(PH_3)_2]^-$ and $[Ti_2Cl_9]^{3-}$ from the *ab initio* CI calculations.

respectively. If there were a strong metal−metal bonding interaction, a single σ bond would be expected between the pair of titanium atoms, and the electronic structure of the Ti(III) compounds might be simply described by a closed-shell singlet ground state (σ^2) with no thermally accessible magnetic excited states. However, as we have seen from their crystal structures, the separation between the Ti(III) centers in all these face-sharing species is approximately 3 Å or greater. At such long distances, the metal−metal interaction, if any, is expected to be so weak such that any Ti−Ti bonding would certainly vanish into magnetic exchange coupling. In the case of antiferromagnetic coupling, the electronic structure would be characterized by a singlet ground state in which both σ and σ^* orbitals would be significantly populated and a triplet first excited state ($\sigma^1\sigma^{*1}$) that should be easily accessible at room temperature. It should be pointed out that, in such a situation, the MO labels, for example, σ and σ^*, merely represent the type of combinations of atomic metal orbitals and are not meant to denote metal−metal bonding or antibonding.

Electronic structures for the two ionic compounds, namely, $[Ti_2Cl_7(PH_3)_2]^-$ and $[Ti_2Cl_9]^{3-}$, at their experimentally observed Ti−Ti distances have been calculated by the *ab initio* CI method. In particular, we calculated not only their ground states but a few low-lying excited states as well. The results of the calculations are entirely consistent with qualitative expectations. For both compounds, the calculations predict a diamagnetic ground state. Notably, the ground state wave functions are dominated by both σ^2 and σ^{*2} configurations with coeffficients 0.77 and −0.61, respectively, in $[Ti_2Cl_7(PH_3)_2]^-$, and 0.75 and −0.64, respectively, in $[Ti_2Cl_9]^{3-}$. Correspondingly, the occupation numbers of the two orbitals obtained from CI natural orbital analysis are also very close, namely, $\sigma^{1.21}\sigma^{*0.78}$ in $[Ti_2Cl_7(PH_3)_2]^-$ and $\sigma^{1.14}\sigma^{*0.85}$ in $[Ti_2Cl_9]^{3-}$. Therefore, as expected, the metal−metal direct σ bonding effect, if any, is completely negligible. Our calculations also show that the first excited state in each compound is a thermally accessible triplet state characterized by the $\sigma^1\sigma^{*1}$ configuration, and is a few hundred wavenumbers in energy above the ground state. This is illustrated clearly in Figure 3 where the relative energies of all calculated electronic states are shown. We may then conclude that there is a significantly strong interaction between the metal centers in these face-sharing bioctahedral complexes but that the dominant nature of the interaction is antiferromagnetic exchange coupling.

It may be mentioned that quantitative results of high accuracy are not expected from the current calculations because of the various approximations and the fixed molecular geometries

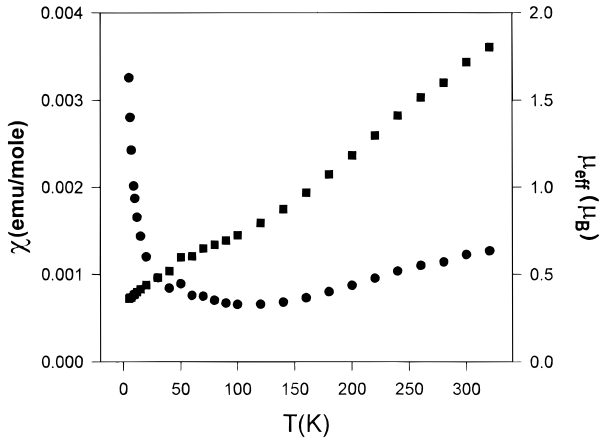

Figure 4. Measured molar magnetic susceptibilities (χ, circles) and effective magnetic moments (μ_{eff}, squares), for $[PPh_4][Ti_2Cl_7(PEt_3)_2]\cdot CH_2Cl_2$.

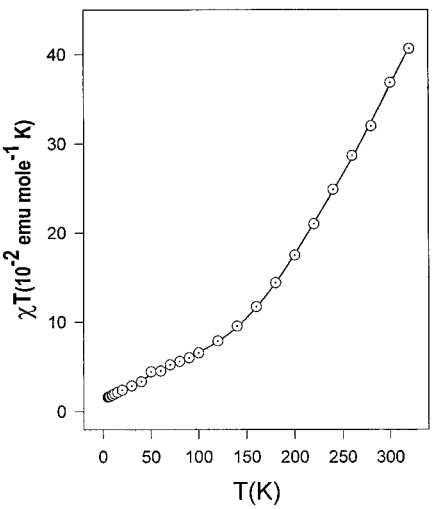

Figure 5. Plot of χT (circles) vs T for $[PPh_4][Ti_2Cl_7(PEt_3)_2]\cdot 2CH_2Cl_2$.

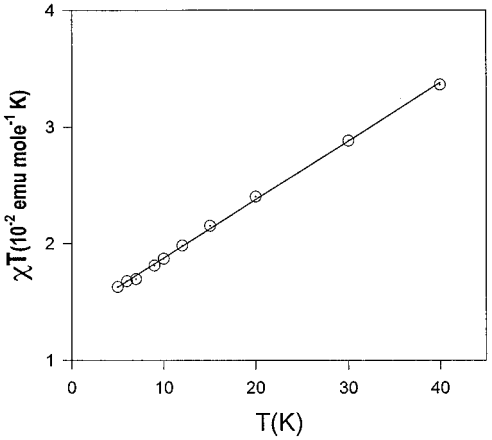

Figure 6. Same as Figure 5 but in the temperature range of 5−40 K.

employed. However, reasonably good or semiquantitative results can still be obtained from these highly reliable, qualitative calculations as can be seen below.

For $[Ti_2Cl_7(PH_3)_2]^-$, the calculated singlet−triplet (S−T) energy separation is 730 cm^{-1}, which is comparable with the value (520 cm^{-1}) obtained from fitting the magnetic data described in the following section. The calculated S−T energy difference, 320 cm^{-1}, for $[Ti_2Cl_9]^{3-}$ is considerably smaller. This may indicate a weaker exchange interaction in this compound that has a much longer Ti−Ti distance (3.19 Å). In addition to the first excited state, a few other low-lying excited states which are shown in Figure 3 were also calculated. In the molcular orbital approach, these states were derived from electronic configurations with one electron in the σ-type orbitals (σ or σ^*) and one electron in the π-type orbitals (π or π^*). The $^{1,3}B_1$ (or $^{1,3}A_2$) states are the lower-energy components of the $^{1,3}E'$ (or $^{1,3}E''$) states as the molecular symmetry is lowered from D_{3h} in $[Ti_2Cl_9]^{3-}$ to C_{2v} in $[Ti_2Cl_7(PH_3)_2]^-$. The energies of these states, relative to the ground state, are in the range of 2360−2520 cm^{-1} in $[Ti_2Cl_7(PH_3)_2]^-$ and 1680−1850 cm^{-1} in $[Ti_2Cl_9]^{3-}$ from the calculations. While they can be regarded as low-lying states in terms of absolute energy, these excited states are too high to be thermally populated. It has been shown, however, that the temperature dependent magnetic behavior of $[Ti_2Cl_9]^{3-}$ can be affected by these excited states through a vibronic coupling mechanism.[7] Such effects may be completely ignored in the case of $[Ti_2Cl_7(PEt_3)_2]^-$, and instead, the excited states may provide a basis for the high values of temperature independent paramagnetism (TIP) of this molecule, as we will see shortly.

The electronic structure of $[Ti_2Cl_9]^{3-}$ has been studied in a number of cases in conjunction with interpretation of its spectroscopic and, in particular, magnetic properties.[7−10] While the $[Ti_2Cl_9]^{3-}$ ion is one of the simplest cases where unquenched orbital momenta are involved in exchange interactions between a pair of metal ions with orbitally degenerate ground state, it is by no means a simple matter to deal theoretically with such interactions. Different theoretical approaches have been proposed[7−9] in which the Hamiltonians are usually heavily parametrized in order to introduce coupling terms that depend not only on spin moments but also on the orbital ones. Although these theoretical models conclude that there is a nonmagnetic ground state, they differ substantially in their predictions of the nature and relative energies of low-lying excited states. The results of our calculations support the arrangement of excited states in this molecule deduced from accurate spectroscopic and magnetic measurements by Kahn and co-workers.[7,10]

Magnetic Properties of $[Ti_2Cl_7(PEt_3)_2]^-$. Figure 4 shows the measured molar magnetic susceptibilities (χ, indicated by circles), corrected for diamagnetism, and the corresponding effective magnetic moment (μ_{eff}, shown by squares), from 5 to 320 K, for $[PPh_4][Ti_2Cl_7(PEt_3)_2]\cdot 2CH_2Cl_2$. The steep rise at very low temperatures is suggestive of a paramagnetic impurity. Above ∼100 K the susceptibility rises uniformly and likewise the effective magnetic moment. It should also be noted that even at the highest temperature (approximately room temperature) the μ_{eff} value has reached only 1.72 μ_B, which is far less than that expected for a pure triplet state. This strongly suggests that the ground state is a singlet but that a triplet state is thermally accessible.

Shown in Figure 5 is the plot of the product of the measured χ and temperature, χT, as a function of T. χT decreases rapidly as T decreases from room temperature towards zero, which is the expected magnetic behavior for an antiferromagnetically coupled dinuclear system. As can be seen, χT is very close to be a linear function of T when $T < 100$ K. In particular, below 40 K, the linearity of χT against T is so good (Figure 6) that χT can be accurately described in terms of a linear equation

$$\chi T = 0.0137 + 501 \times 10^{-6}\mathrm{T} \qquad (1)$$

where the unit of χT is emu·mol^{-1}·K. Therefore, χT ($T \rightarrow 0$) = 0.0137 represents contributions due to the paramagnetic impurity, and we may correctly assume that the magnetic behavior of the impurity is governed by $\chi_{imp} = 0.0137/T$ without necessarily knowing its actual nature. The second term on the right side of eq 1, on the other hand, gives rise to a temperature-independent contribution to χ, and we may write $\chi_{TIP} = 501 \times 10^{-6}$ emu/mol.

Before attempting to fit the measured data with a theoretical model, a few other points must be considered. We note that the appearance of χT vs T as shown in Figure 5 is similar to the behavior of χT for $[Ti_2Cl_9]^{3-}$.[7] It is well known[7-10] that the magnetic interactions in $[Ti_2Cl_9]^{3-}$ involve two metal centers of high symmetry that have unquenched orbital angular momenta. It has also been indicated that a more complete description of thermal variation of χ in this case should also include the effects of the high-energy states of a trigonally distorted T_{2g} level that could be vibronically coupled to the lowest-energy state.[7] For $[Ti_2Cl_7(PEt_3)_2]^-$, however, substitution of a Cl atom in a $TiCl_6$ unit by a phosphine ligand leads to a lower symmetry at a local metal site and overall lower symmetry of the dinuclear system. Because of the low symmetries and a stronger metal−metal interaction as revealed by the electronic structure calculations, we may assume that the first-order orbital momenta should have only negligible effects on the magnetic properties of $[Ti_2Cl_7(PEt_3)_2]^-$. We also tend to believe that possible effects of any vibronically coupled excited states could be reasonably neglected in the case of our phosphine compound because of the apparent larger energy gaps between the ground state and the excited states of A_2 and B_1 symmetries (Figure 3). Furthermore, as in the case of $[Ti_2Cl_9]^{3-}$,[7] we may also discount any magnetic contributions due to spin-orbit coupling.

The exchange interaction between the two d^1 metal centers, therefore, may be formulated as a spin-only case by a Hamiltonian of the form

$$\mathbf{H} = -J\mathbf{S_A}\cdot\mathbf{S_B} \qquad (2)$$

where J is the exchange coupling constant. Correspondingly, the magnetic susceptibility (χ_0) due to thermal distribution over both the singlet ground state and the triplet first excited state for such a system may be expressed by using the van Vleck equation[16] as follows

$$\chi_0 = (2Ng^2\beta^2/kT)\,[3 + \exp(-J/kT)]^{-1} \qquad (3)$$

where N, g, β, and k have their usual meanings, and -J is the S−T energy difference.

The measured molar susceptibilities may be given by the expression

$$\chi = (1 - \alpha)\chi_0 + \chi_{imp} + \chi_{TIP} \qquad (4)$$

in which α is the molar fraction of the paramagnetic impurity. Since α is surely a very small number, it can be safely neglected in the following fitting procedure. Thus, by using the results for χ_{imp} and χ_{TIP} from eq 1, and the expression for χ_0 in eq 3, the measured molar susceptibilities as a function of temperature were fitted to eq 5, by using a least-squares procedure

$$\chi = (2Ng^2\beta^2/kT)\,[3 + \exp(-J/kT)]^{-1} + 0.0137/T + 501 \times 10^{-6} \qquad (5)$$

It may be noted that there is virtually only one fitting parameter, namely, the coupling constant J in eq 5.

The results of this fitting procedure are very satisfactory, as illustrated in Figure 7, where the curve fitting converged with $-J = 524$ cm^{-1}, with g in eq 5 set to 2. In the figure, the fitted results for χ are displayed by the solid line passing through the circles (measured data). The solid line passing through the squares is the corresponding result for the effective magnetic moments (μ_{eff}). We may also take g as a parameter into the fitting. When this was done, we found $-J = 552$ cm^{-1}, $g = 2.15$, and an even better fit of χ to the measured data, as can be seen clearly in Figure 8. Therefore, we conclude that all our previous assumptions that have led to the spin-only interpretation must be esssentially correct.

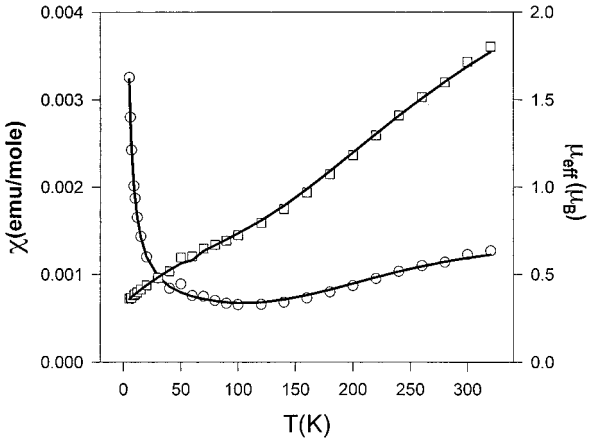

Figure 7. Results of least-squares fitting for χ (solid line) using eq 5 with g fixed at 2 for $[PPh_4][Ti_2Cl_7(PEt_3)_2]\cdot 2CH_2Cl_2$.

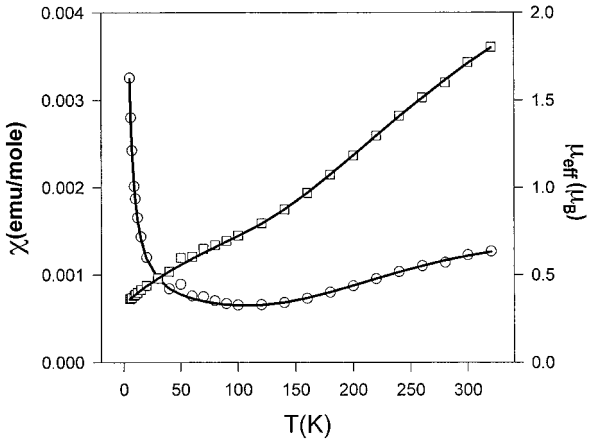

Figure 8. Same as Figure 7 but with g also as a fitting parameter.

Finally, it may be noted that the value for χ_{TIP} as obtained from eq 1 is significantly greater than those, namely, $\sim 100 \times 10^{-6}$ emu/mol, observed in many mononuclear species[10] and in the dinuclear species, $[Nb_2Cl_7(PR_3)_2]^-$.[15] The manifestation of TIP in a molecular system characterized by a spin singlet ground state is a typical second-order reponse property[17] and, as such, is sensitive to the spectrum of excited states. The TIP can be large if there exist accessible but not thermally populated low-lying excited states.[16] As can be seen in Figure 3, these conditions are well satisfied by the electronic structure of $[Ti_2Cl_7(PR_3)_2]^-$.

Acknowledgment. We thank the National Science Foundation for support, and the Supercomputer Center at Texas A&M University for granting computer time. SQUID data were obtained in the Physics Department at Michigan State University which was supported, in part, by the National Science Foundation and Michigan State University Center for Fundamental Materials Research.

Supporting Information Available: An X-ray crystallographic file of compounds **1**·$2CH_2Cl_2$ and **2**·CH_2Cl_2 in CIF format is available on the Internet. Access information is given on any current masthead page.

IC960636K

(17) Buckingham, A. D.; *Adv. Chem. Phys.* **1967**, *12*, 107.